

**Quasi-steady-state analysis of coupled flashing ratchets**

Ethan Levien and Paul C. Bressloff\*

*Department of Mathematics, University of Utah, 155 South 1400 East, Salt Lake City, Utah 84112, USA*

(Received 29 May 2015; revised manuscript received 4 September 2015; published 12 October 2015)

We perform a quasi-steady-state (QSS) reduction of a flashing ratchet to obtain a Brownian particle in an effective potential. The resulting system is analytically tractable and yet preserves essential dynamical features of the full model. We first use the QSS reduction to derive an explicit expression for the velocity of a simple two-state flashing ratchet. In particular, we determine the relationship between perturbations from detailed balance, which are encoded in the transitions rates of the flashing ratchet, and a tilted-periodic potential. We then perform a QSS analysis of a pair of elastically coupled flashing ratchets, which reduces to a Brownian particle moving in a two-dimensional vector field. We suggest that the fixed points of this vector field accurately approximate the metastable spatial locations of the coupled ratchets, which are, in general, impossible to identify from the full system.

DOI: [10.1103/PhysRevE.92.042129](https://doi.org/10.1103/PhysRevE.92.042129)

PACS number(s): 05.40.Jc, 87.10.-e

**I. INTRODUCTION**

Noise-driven transport phenomena in spatially periodic systems are a fundamental feature of many physical processes, particularly in cell biology [1]. Mathematically speaking, these processes are often modeled in terms of a Brownian particle subject to a spatially periodic potential energy environment. There are at least two distinct mechanisms by which such a system can be driven away from equilibrium and produce mechanical work. The first, which we will refer to as a Brownian particle in an effective potential, involves a constant external force resulting in an effective potential that is tilted periodic, which means it is more probable that the Brownian particle escapes the potential barrier on one side [2]. On the other hand, in the case of a flashing ratchet, the particle undergoes a set of conformational changes that affect how it interacts with some underlying periodic structure and perturbations from equilibrium are encoded in the transitions rates between the conformational states. In this case, directional transport can occur when the transition rates do not satisfy detailed balance [3–5].

Both the flashing and Brownian particle evolving in effective potentials have rich histories in theoretical studies of biochemistry and intracellular transport. For example, these models have been used to gain qualitative insight into the dynamics of molecular motors [6–10]. Molecular motors constitute a wide range of nanoscale machines that are able to convert chemical energy, often in the form of ATP, into mechanical work by cycling through a number of conformational states [11]. Examples include flagellar motors that provide locomotion for single-celled organisms and cytoskeletal motors that perform a number of tasks by “walking” along polymerized filaments within cells. A flagellar motor consists of a set of torque generating stator proteins, which change conformation in response to an electrochemical gradient [12], whereas a cytoskeletal motor like kinesin or dynein has multiple “legs” that attach and detach to polymerized filaments as a result of chemical reactions [11].

The two-state flashing ratchet, which we will examine in this paper, was first analyzed by Prost *et al.* [3]. Motivated by applications to molecular motors, they investigated how the spatial structure of perturbations from detailed balance related to the pumping of particles in a flashing ratchet. Subsequent studies by Prost and co-workers analyzed large systems of coupled flashing ratchets [6,13–15]. A major focus of these studies was on self-organization in mean field models, since systems of flashing ratchets are usually analytically intractable. As a result, some information about motor interactions is lost. (For a recent review of other approaches to modeling cooperative effects in systems of molecular motors see Ref. [16].)

Analysis of Brownian particles in effective potentials is more straightforward and they too have a rich history in the context of molecular motors and intracellular transport. For example, Peskin and Elston gave theoretical evidence that motor cargo coupling is elastic [17]. Other more mathematical studies of Brownian particles explore topics such as stochastic resonance and coherence in molecular motors [18]. Similar results for flashing ratchets would be difficult to obtain using standard tools due to the hybrid nature of these systems.

In this paper we establish a connection between Brownian particles in effective potentials and flashing ratchets by carrying out a quasi-steady-state (QSS) or adiabatic reduction, in which the discrete-state transitions in a flashing ratchet are absorbed into the deterministic part of the stochastic process, resulting in an effective tilted-periodic potential for a Brownian particle. It has been established rigorously that this reduction is valid for a stochastic hybrid system as the transitions rates become large [19]. Although the QSS approximation has previously been used within the context of molecular motors [20], we are not aware of an instance in which it has been applied to a flashing ratchet. This is possibly due to the fact that the fast transition-rate limit does not necessarily hold for biological molecular motors at the length scales and time scales associated with single steps. (On the other hand, at the larger scale of successive runs of a molecular motor, transitions between runs can be treated as relatively fast [21,22].) Here we propose that the QSS reduction be used not as a means for accurately approximating the probability density of the system, but for obtaining qualitative information about the flashing

\*bressloff@math.utah.edu

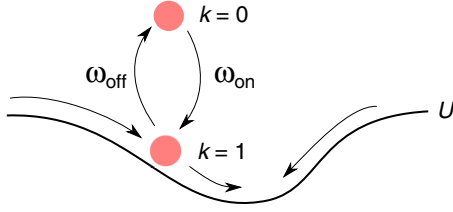


FIG. 1. (Color online) Diagram of the two-state flashing ratchet.

ratchet, which would be difficult to obtain otherwise. We first review the standard analysis of flashing ratchets and show how the numerical results obtained in Ref. [3] can be derived analytically from the QSS reduction. We then explore a pair of elastically coupled flashing ratchets and show that the QSS reduction allows us to predict the metastable states of the full system, as well as its mean velocity. The system of two coupled ratchets has previously been studied numerically in Ref. [10], although their focus is on the probability current rather than the identification of metastable states.

## II. FLASHING RATCHET

We begin by reviewing the theory of flashing ratchets; for a more detailed introduction see Refs. [1,3,6,23]. In the most general type of flashing ratchet, a particle switches stochastically between a finite set of discrete states according to space-dependent transition rates. In each state the motor evolves as a Brownian particle in a potential. Here we will restrict our attention to the two-state flashing ratchet, where a motor can be in either an attached state ( $k = 1$ ) in which it is sensitive to a periodic potential  $U(x)$  of period  $\ell$  or a detached state ( $k = 0$ ) in which it diffuses freely in the environment (see Fig. 1). In the attached state, the location  $x$  of the particle evolves according to the Langevin equation

$$dx = -\frac{U'(x)}{\gamma}dt + \sqrt{2D}dW(t),$$

where  $W(t)$  is a Wiener process,  $D$  is the diffusion coefficient, and  $\gamma$  is the friction coefficient with  $D\gamma = k_B T$ . Let  $p_1(x, t)$  and  $p_0(x, t)$  be the probability that at time  $t$  the particle is at position  $x$  and in the attached and detached states, respectively. The corresponding Chapman-Kolmogorov equation for the probability vector  $\mathbf{p}(x, t) = (p_0, p_1)$  is

$$\frac{\partial}{\partial t} p_0 + \frac{\partial}{\partial x} J_0 = -\omega_{\text{on}}(x)p_0 + \omega_{\text{off}}(x)p_1, \quad (1a)$$

$$\frac{\partial}{\partial t} p_1 + \frac{\partial}{\partial x} J_1 = \omega_{\text{on}}(x)p_0 - \omega_{\text{off}}(x)p_1, \quad (1b)$$

where the fluxes  $J_0$  and  $J_1$  are given by

$$J_0 = -D\frac{\partial}{\partial x} p_0, \quad J_1 = -\frac{U'(x)}{\gamma}p_1(x, t) - D\frac{\partial}{\partial x} p_1(x, t).$$

We consider the solutions  $\mathbf{p}(x, t)$ , which are defined on  $\mathbb{R} \times \mathbb{R}^+$  and for which the total probability  $u(x, t) = p_0 + p_1$  satisfies the normalization condition

$$\int_{\mathbb{R}} u(x, t) dx = 1.$$

The standard analysis of the system (1) proceeds as follows. First we define the reduced densities and fluxes

$$\hat{p}_j = \sum_{n=-\infty}^{\infty} p_j(x + n\ell, t), \quad \hat{J}_j = \sum_{n=-\infty}^{\infty} J_j(x + n\ell, t).$$

It follows from linearity that  $(\hat{p}_0, \hat{p}_1)$  satisfies Eq. (1) and may be normalized in the interval  $[0, 1]$ . Next we consider the total probability  $\hat{u}(x, t) = \hat{p}_0 + \hat{p}_1$ , which has the corresponding probability flux

$$\hat{J}(x, t) = -\frac{U'(x)}{\gamma}\hat{p}_0(x, t) - D\frac{\partial \hat{u}(x, t)}{\partial x}.$$

Unlike the probabilities in the original system, the reduced probability  $\hat{u}$  will converge to a unique steady state  $\hat{u}^{\text{SS}}$  with constant probability flux  $\hat{J}^{\text{SS}}$ . It can be shown that the average velocity of a particle depends on the probability flux according to

$$v = \int_0^\ell \hat{J}(x) dx = \hat{J}^{\text{SS}} \ell. \quad (2)$$

Upon analyzing this system one finds that unless the detailed balance condition  $\omega_{\text{on}}(x)/\omega_{\text{off}}(x) = e^{-U(x)/k_B T}$  breaks down, the system will have a zero steady-state flux and hence  $v = 0$ . There is a great deal of interest in understanding how the spatial structure of deviations from detailed balance affect the motor velocity.

Deviation or perturbation from detailed balance is usually measured by the quantity

$$\Omega(x) = \omega_{\text{on}}(x) - \omega_{\text{off}}(x)e^{U(x)/k_B T}. \quad (3)$$

When  $\Omega(x) = 0$ , one can easily check that the transition rates satisfy detailed balance or, alternatively, that the probabilities of occupying the on and off states are given by a Boltzmann distribution. For simple transition rates and potential one can obtain results about how the function  $\Omega(x)$  relates to the velocity. In particular, for piecewise linear dynamics it has been established that in the limiting case in which perturbations from detailed balance are localized the velocity is a monotonically increasing function of  $\bar{\Omega} = \int_0^1 \Omega(x) dx$ , while nearly homogenous perturbations yield a unimodal function for which  $v \rightarrow 0$  as  $\bar{\Omega} \rightarrow \infty$  [3].

While it is difficult to say much about the behavior of an arbitrary flashing ratchet, a Brownian particle evolving in a single potential is analytically tractable. The flashing ratchet can be related to an effective potential by carrying out a QSS reduction. This proceeds as follows. Assume that the transitions are sufficiently fast (see below) so that at each point  $x$  on very short time scales the probability vector  $\hat{\mathbf{p}} = (\hat{p}_0, \hat{p}_1)$  converges to the space-clamped steady state  $\boldsymbol{\rho} = (\rho_0, \rho_1)$  with

$$\rho_0(x) = \frac{\omega_{\text{off}}(x)}{\omega_{\text{on}}(x) + \omega_{\text{off}}(x)}, \quad \rho_1(x) = \frac{\omega_{\text{on}}(x)}{\omega_{\text{on}}(x) + \omega_{\text{off}}(x)}.$$

Then define the effective velocity  $v(x)$  to be the velocity due to the potential  $U(x)$  weighted by the probability that the motor is in the attached state, that is,  $v(x) = -U'(x)\rho_1(x)/\gamma$ . Hence in the limit of fast transition rates  $\hat{\mathbf{p}}(x, t)$  evolves as a Brownian

particle according to

$$\begin{aligned} \frac{\partial}{\partial t} \hat{u}(x,t) + \frac{\partial}{\partial x} \hat{J}_q(x,t) &= 0, \\ \hat{J}_q(x,t) &= -\frac{U'_q(x)}{\gamma} \hat{u}(x,t) - D \frac{\partial}{\partial x} \hat{u}(x,t) \end{aligned}$$

with an effective potential

$$U_q(x) = -\gamma \int_0^x v(y) dy = \int_0^x U'(y) \rho_1(y) dy.$$

At steady state  $\hat{J}_q(x,t) = \hat{J}_q^{\text{SS}}$  is constant and solving for  $\hat{u}_q^{\text{SS}}$  using an integrating factor yields

$$\begin{aligned} \hat{u}_q^{\text{SS}}(x) &= \frac{\hat{J}_q^{\text{SS}} Z(x)}{1 - e^{-\{U_q(y)\}_{y=0}^\ell / k_B T}}, \\ Z(x) &= \frac{1}{D} e^{-U_q(x)/k_B T} \int_x^{x+\ell} e^{U_q(x')/k_B T} dx'. \end{aligned}$$

The normalization condition is then used to solve for  $\hat{J}_q^{\text{SS}}$  so that Eq. (2) becomes

$$v = \frac{\ell [1 - e^{-\{U_q(y)\}_{y=0}^\ell / k_B T}]}{\int_0^\ell Z(x') dx'}. \quad (4)$$

A necessary condition for the effective potential to generate motion is that  $U_q(\ell) \neq U_q(0)$ , that is,  $U_q(x)$  is not  $\ell$  periodic.

It remains to specify more explicitly the conditions under which the QSS reduction is valid. In dimensional variables, if  $\ell = 10$  nm and  $D = 1 \mu\text{m}^2 \text{s}^{-1}$  [24], the fundamental unit of time is  $10^{-2}$  s. A molecular motor such as kinesin makes around 100 steps per second, suggesting that the transition rates in Eq. (1) are at least of order  $10^2 \text{s}^{-1}$ . Therefore, we will assume  $10^2 \text{s}^{-1} \leq \omega_{\text{on}}, \omega_{\text{off}} \leq 10^4 \text{s}^{-1}$  [24] or, in dimensionless units,  $1 \leq \omega_{\text{on}}, \omega_{\text{off}} \leq 100$ . For the moment, suppose that the dimensionless transition rates are in the range 10–100. This motivates the introduction of a scaling factor  $\epsilon$  such that  $\omega_{\text{on}}, \omega_{\text{off}} \rightarrow \omega_{\text{on}}/\epsilon, \omega_{\text{off}}/\epsilon$  with the rescaled transition rates independent of  $\epsilon$ . It can then be proved rigorously that  $\hat{u}_q^{\text{SS}}$  is an exact steady-state solution for the total probability of the full system in the limit  $\epsilon \rightarrow 0$  [19]. Moreover, for  $0 < \epsilon \ll 1$ , the QSS reduction generates an  $O(\epsilon)$  correction to the diffusion coefficient  $D$  [21], which can be ignored, and the QSS solution is still a reasonable approximation. Throughout the rest of the paper we use the nondimensionalize variables  $\ell = 1$  and  $D = 1$ . We also set the attachment rate to be constant  $\omega_{\text{on}} = \epsilon^{-1}$  and express the detachment rate in terms of the detailed balance relation

$$\omega_{\text{off}}(x) = \epsilon^{-1} [\Omega(x) + e^{U(x)/k_B T}],$$

where we have also rescaled  $\Omega(x)$  by  $\epsilon^{-1}$ . This simplifies matters because the transition rates are completely defined by  $U(x)$  and  $\Omega(x)$ . Figure 2 displays the QSS potential  $U_q(x)$  for  $U(x)$  given by a periodic sawtooth function or a sinusoid. In order for the effective potential  $U_q(x)$  to be tilted, the perturbations from detailed balance must be symmetric. For a piecewise potential

$$U(x) = U^*[(1 - x/a)H(a - x) + (x/a - 1)H(x - a)],$$

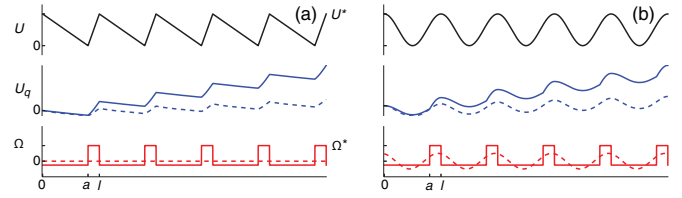


FIG. 2. (Color online) (a) Periodic piecewise linear potential (top), perturbations from detailed balance (bottom), and corresponding effective potential  $U_q$ . The solid curve for  $\Omega$  represents a localized perturbation from detailed balance while the dashed curve represents an approximately uniform perturbation. We set  $\ell = 1$  throughout. For the localized case,  $\Omega(x) = (1/a)\bar{\Omega}$  when  $a < x < 1$  and 0 otherwise. For the quasiuniform case,  $\Omega(x) = \bar{\Omega}$ . (b) Corresponding figures for a sinusoidal potential. The quasiuniform perturbation is now taken to be  $\Omega(x) = \cos(2\pi x) + \bar{\Omega}$ .

with  $a \neq 1/2$  and  $H(x)$  the Heaviside function, the potential itself is asymmetric so even with constant  $\Omega$  the effective potential is tilted, as can be seen in Fig. 2(a). On the other hand, for the sinusoidal potential, constant transition rates would not produce a tilted potential since  $U$  is symmetric. Instead we have shown a sinusoidal potential with a small phase offset and it can be seen in Fig. 2(b) that this does indeed produce a tilted effective potential.

We now derive the relationship between  $\bar{\Omega}$  and  $v$  as follows. First, write  $\rho_1(x)$  in terms of  $\Omega(x)$ :

$$\rho_1(x) = [1 + e^{U(x)/k_B T} + \Omega(x)]^{-1}.$$

When the perturbations are nearly uniform,  $\Omega(x) \approx \bar{\Omega}$  for all  $x$ . Hence, in the limit  $\bar{\Omega} \rightarrow \infty$ , we have  $\rho_1(x) \rightarrow 0$  and thus  $U_q(x) \rightarrow 0$ . It follows that  $v \rightarrow 0$  when  $\bar{\Omega} \rightarrow \infty$ . [Note that we could have fixed  $\omega_{\text{off}}(x) = 1$ , so that  $\rho_1(x) \rightarrow 1$  and  $U_q(x) \rightarrow U(x)$  as  $\bar{\Omega} \rightarrow \infty$  and still  $v \rightarrow 0$ , since  $U(x)$  is periodic.] On the other hand, if perturbations are localized around an end point, say,  $x = 0$ , then in the limit  $\bar{\Omega} \rightarrow \infty$ ,  $\rho_1(0) = 0 \neq \rho_1(l)$  and  $v \neq 0$ . In Fig. 3 we plot the velocity  $v$  of Eq. (4) as a function of  $\bar{\Omega}$ . It can be seen that the QSS velocity's dependence on the deviation from detailed balance is

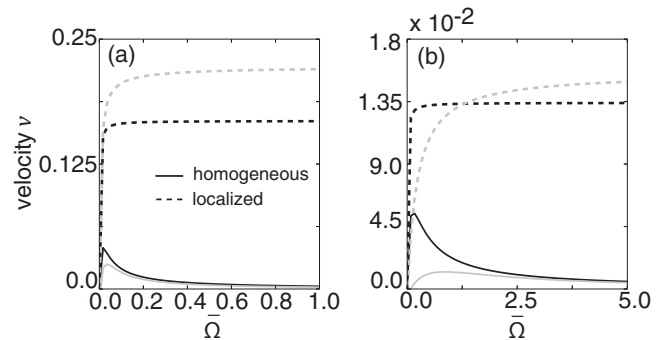


FIG. 3. Plot of flashing ratchet velocity  $v$  as a function of  $\bar{\Omega}$  using piecewise linear transitions rates and potentials (see Fig. 2) for (a)  $\epsilon = 0.01$  and (b)  $\epsilon = 1$ . Solid (dashed) curves correspond to a quasiuniform (localized) perturbation  $\Omega(x)$ . The solutions of the flashing ratchet model are given by the gray curves and the solutions of the reduced model are given by the black curves. The parameter values are  $D = 1$ ,  $\ell = 1$ , and  $a = 0.4$ .

in qualitative agreement with that of the full system even when  $\epsilon = 0.1$ . Consistent with the findings of Ref. [3], the velocity is a monotonically increasing function of  $\overline{\Omega}$  for a localized perturbation and a unimodal function of  $\overline{\Omega}$  for a quasiuniform perturbation.

### III. PAIR OF ELASTICALLY COUPLED FLASHING RATCHETS

We next consider a system of two elastically coupled flashing ratchets with possibly different dynamical properties. While many studies have analyzed collective behavior in mean field models of coupled ratchets [6,13–15], there are very few analytical results concerning the effects of coupling on small numbers of flashing ratchets. One problem is that for small numbers of coupled particles the assumption that coupling is rigid breaks down, which greatly increases the complexity of the calculations. Note that each ratchet can be interpreted as a molecular motor [25,26] or as the head of a single two-headed motor [10].

Extending the ideas applied to the single flashing ratchet, we will show how the QSS reduction can be used to gain insight into the dynamics of elastically coupled flashing ratchets, which are analytically intractable for even the simplest choices of rate functions and potentials. In this model each motor is associated with an  $\ell$ -periodic potential  $U_i(x_i)$  and rate functions  $\omega_{\text{on}}^{(i)}(x_i)$  and  $\omega_{\text{off}}^{(i)}(x_i)$  describing the rate of attaching and detaching from the potential, respectively;  $x_i$  is the spatial position of the  $i$ th motor. One simplifying assumption is that the transition rates depend only on the position of a single motor, hence strain-dependent unbinding has been neglected [25]; this assumption has also been applied to two coupled heads of a single motor [10]. We take the tethers to be Hookean

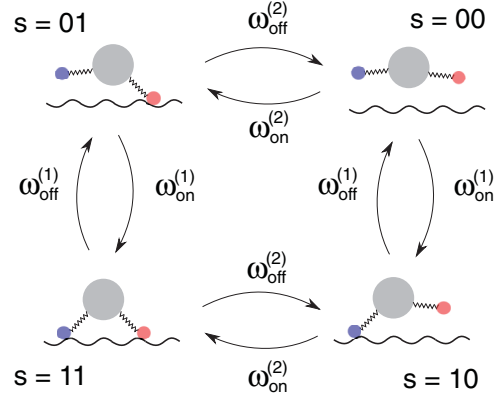


FIG. 4. (Color online) Diagram of the discrete internal state space for two coupled flashing ratchets.

so that the elastic energy of the system is

$$U_{\text{spring}}(\mathbf{x}) = \frac{1}{2}\kappa(x_1 - x_2 - z)^2,$$

where  $z$  is the equilibrium position of the spring.

The discrete internal states of the system are elements of the set  $S = \{00, 01, 10, 11\}$  (see Fig. 4). We start by writing down the Chapman-Kolmogorov equation for the probability  $p_s(\mathbf{x}, t)$  that the system is in state  $s \in S$  with motor position  $\mathbf{x} = (x_1, x_2)$  at time  $t$ . We use  $s_i \in \{0, 1\}$  to denote the state of the  $i$ th motor; for example, in the state  $s = 10$ , motor 1 is in state  $s_1 = 1$ . Given the above assumptions, the probability vector  $\mathbf{p}(\mathbf{x}, t) = (p_{00}, p_{01}, p_{10}, p_{11})$  evolves according to

$$\frac{\partial}{\partial t} \mathbf{p} = -\frac{\partial}{\partial x_1} V_1 \mathbf{p} - \frac{\partial}{\partial x_2} V_2 \mathbf{p} + D \nabla^2 \mathbf{p} + \frac{1}{\epsilon} A(\mathbf{x}, t) \mathbf{p},$$

where

$$A(\mathbf{x}, t) = \begin{pmatrix} -\omega_{\text{on}}^{(1)}(x_1) - \omega_{\text{on}}^{(2)}(x_2) & \omega_{\text{off}}^{(2)}(x_2) & \omega_{\text{off}}^{(1)}(x_1) & 0 \\ \omega_{\text{on}}^{(2)}(x_2) & -\omega_{\text{off}}^{(2)}(x_2) - \omega_{\text{on}}^{(1)}(x_1) & 0 & \omega_{\text{off}}^{(1)}(x_1) \\ \omega_{\text{on}}^{(1)}(x_1) & 0 & -\omega_{\text{off}}^{(1)}(x_1) - \omega_{\text{on}}^{(2)}(x_2) & \omega_{\text{off}}^{(2)}(x_2) \\ 0 & \omega_{\text{on}}^{(1)}(x_1) & \omega_{\text{on}}^{(2)}(x_2) & -\omega_{\text{off}}^{(1)}(x_1) - \omega_{\text{on}}^{(2)}(x_2) \end{pmatrix}$$

and  $V_1$  has diagonal entries

$$v_s^{(1)}(\mathbf{x}) = -\kappa(x_1 - x_2 - z) + f_1(x_1)s_1,$$

while  $V_2$  has diagonal entries

$$v_s^{(2)}(\mathbf{x}) = \kappa(x_1 - x_2 - z) + f_2(x_2)s_2$$

with  $f_i(x_i) = -U_i'(x_i)/\gamma$ . Observe that  $\mathbf{v}_s(\mathbf{x}) = [v_s^{(1)}(\mathbf{x}), v_s^{(2)}(\mathbf{x})]^T$  is the gradient of a two-dimensional scalar potential. Hence, in any given state we can think of the motor pair as a single Brownian particle moving in the two-dimensional potential

$$U_s^{\text{tot}}(\mathbf{x}) = \frac{1}{2}\kappa(x_1 - x_2 - z)^2 + U_1(x_1)s_1 + U_2(x_2)s_2,$$

with  $\mathbf{v}_s(\mathbf{x}) = -\nabla U_s^{\text{tot}}(\mathbf{x})/\gamma$ . In the remainder of this paper we often refer to  $\mathbf{x}$  as a single particle evolving in a two-dimensional spatial domain. This interpretation is advantageous because it relates the coupled model to a two-dimensional flashing ratchet.

To illustrate the utility of the QSS reduction we first consider a system for which the center of mass has zero velocity. (Nonzero velocities are considered later.) To do this we consider the simple case in which each particle moves in the same sinusoidal potential  $U$  and has the same sinusoidal perturbation  $\Omega$  from detailed balance [see Fig. 2(b)]. The only difference is that the sinusoidal functions of the first motor are out of phase by  $1/4$  with respect to the second particle. In other words,  $U_2(x) = U_1(x - 1/4)$  and  $\Omega_2(x) = \Omega_1(x - 1/4)$ . Shifting the phase of the potentials ensures that the advection terms for the two particles do not share the same zeros. As we will soon see, this makes the identification of metastable spatial positions nontrivial and motivates the application of the QSS reduction.

Let us begin by noting that in the limit  $\kappa \rightarrow \infty$  the effective Brownian particle moves along the line  $x_2 = x_1$ , hence the distance between the motors is fixed and they move synchronously in one dimension. Decreasing  $\kappa$  should



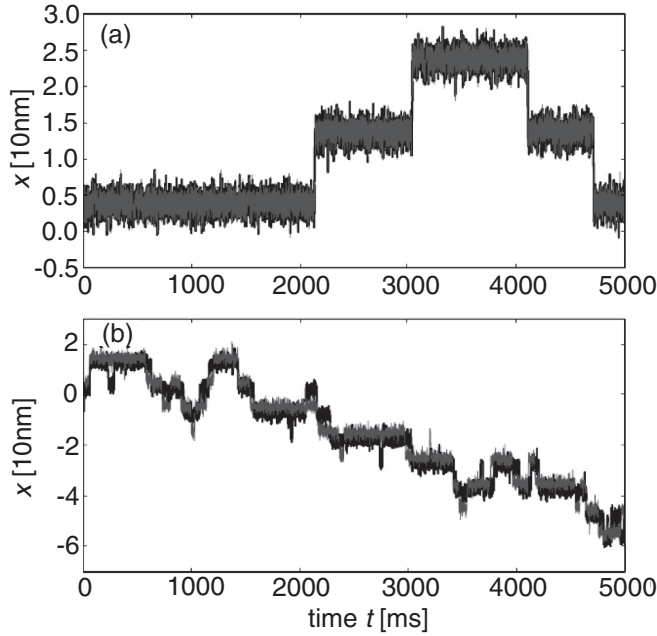


FIG. 5. Stochastic trajectories  $x = x_1, x_2$  of the two particles (indicated by black and gray lines, respectively) with deterministic dynamics corresponding to (a) a hard spring ( $\kappa = 8$ ) and (b) a soft spring ( $\kappa = 0.1$ ). Other parameters are  $D = 1$ ,  $z = 0$ , and  $\varepsilon = 1$ . Trajectories were generated by running a forward Euler method on the SDE for the current state and calculating the time until the next state transition. If the time is less than the time step  $dt = 0.01$ , then a random number is generated to select a state transition.

introduce metastable points off the line  $x_1 = x_2$ , which increases the number of stable configurations we observe and hence increases the variance in motor position. This effect can be seen in numerical simulations (see Fig. 5). Note that the system seems to spend most of its time with the particles close together, although not at the exact same spatial position. This behavior is reminiscent of the common modeling approach in which space is discretized and the various motor configurations are characterized by the elastic energy between the two motors [25–27]. In contrast to previous work on coupled ratchets, we do not assume that the discrete energy states are located at regular intervals on a lattice; instead we want to determine their location by analyzing the flashing ratchet system.

Figures 6 and 7 show the four vector fields  $\mathbf{v}_s(\mathbf{x})$ ,  $s \in \{00, 01, 10, 11\}$ , for two different values of the spring constant  $\kappa$  and  $z = 0$ . It is tempting to relate these figures to the different transport regimes observed in Fig. 5, but it is not immediately clear what information about the system can be extracted from these vector fields. In the absence of state transitions, fixed points of these vector fields are metastable states of the corresponding continuous stochastic process for that state. However, in the stochastic hybrid system the particle does not necessarily have time to converge to one of these metastable locations and once it arrives it may transition to a state where the same location is not metastable. In this example, we have explicitly chosen potentials that do not share the same fixed points. Therefore, it is not clear whether or not any metastable states exist and if they do, whether or not they coincide with those of any of the individual states. In fact, even if

all potentials share the same fixed points and their basins of attraction coincide, it is possible that the location of the fixed points may not correspond to a metastable location in the full system [28].

In order to make meaningful statements about the dynamics of the coupled ratchet system, one must determine how to incorporate information about the transition rates and establish how the individual potentials relate to the dynamics of the full system. For problems in which noise is weak, a WKB approximation can be used to construct a quasipotential, which accurately approximates the evolution of a particle in the stochastic hybrid system [29]. Unfortunately, the WKB approximation can be difficult to construct and is not appropriate for the flashing ratchet where diffusion acts as a strong source of noise. We now demonstrate how the QSS reduction can be used to obtain an effective two-dimensional system that contains much of the information about the full model we are interested in.

As in the single ratchet case, when the switching is relatively fast ( $\varepsilon \rightarrow 0$ ), the probability density will converge to a unique steady-state density  $\rho$  at each  $\mathbf{x}$ , which satisfies  $A\rho = 0$ . In this limit we derive a scalar Fokker-Planck (FP) equation for the total probability

$$u(\mathbf{x}, t) = \sum_{s \in S} p_s(\mathbf{x}, t),$$

which is subject to the normalization condition

$$\int_{\mathbb{R}^2} u(\mathbf{x}, t) d\mathbf{x} = 1.$$

The effective velocity for  $u$  is given by weighting each velocity vector  $\mathbf{v}_s = (v_s^{(1)}, v_s^{(2)})^T$  by the probability that the system is in state  $s$ , so we have

$$\mathbf{v}(\mathbf{x}) = \sum_{s \in S} \rho_s(\mathbf{x}) \mathbf{v}_s(\mathbf{x}).$$

Neglecting  $O(\varepsilon)$  terms, the FP equation for  $u$  is

$$\frac{\partial u}{\partial t} = -\nabla \cdot [\mathbf{v}(\mathbf{x})u] + D\nabla^2 u. \quad (5)$$

After some computation we find that the QSS velocity of the  $i$ th motor is given by

$$v_i(\mathbf{x}) = (-1)^i \kappa (x_1 - x_2 - z) + f_i(x_i) \sigma_i(x_i), \quad (6)$$

where

$$\sigma_i(x_i) = \frac{\omega_{\text{on}}^{(i)}(x_i)}{\omega_{\text{on}}^{(i)}(x_i) + \omega_{\text{off}}^{(i)}(x_i)}. \quad (7)$$

Following the analysis of the single ratchet, let  $\Omega_1(x)$  and  $\Omega_2(x)$  measure the perturbations from detailed balance of the two motors. Specifically,

$$\Omega_i(x) = \omega_{\text{on}}^{(i)}(x) - \omega_{\text{off}}^{(i)}(x) e^{U_i(x)/k_B T}.$$

Taking  $\omega_{\text{on}}^{(i)}(x) = 1$ , we have

$$\sigma_i(x) = [1 + e^{U_i(x)/k_B T} + \Omega_i(x)]^{-1}.$$

In general, it is more difficult to interpret the dynamics of a particle in a two-dimensional vector field resulting from the QSS of the coupled ratchets because  $\mathbf{v}(\mathbf{x})$  is not

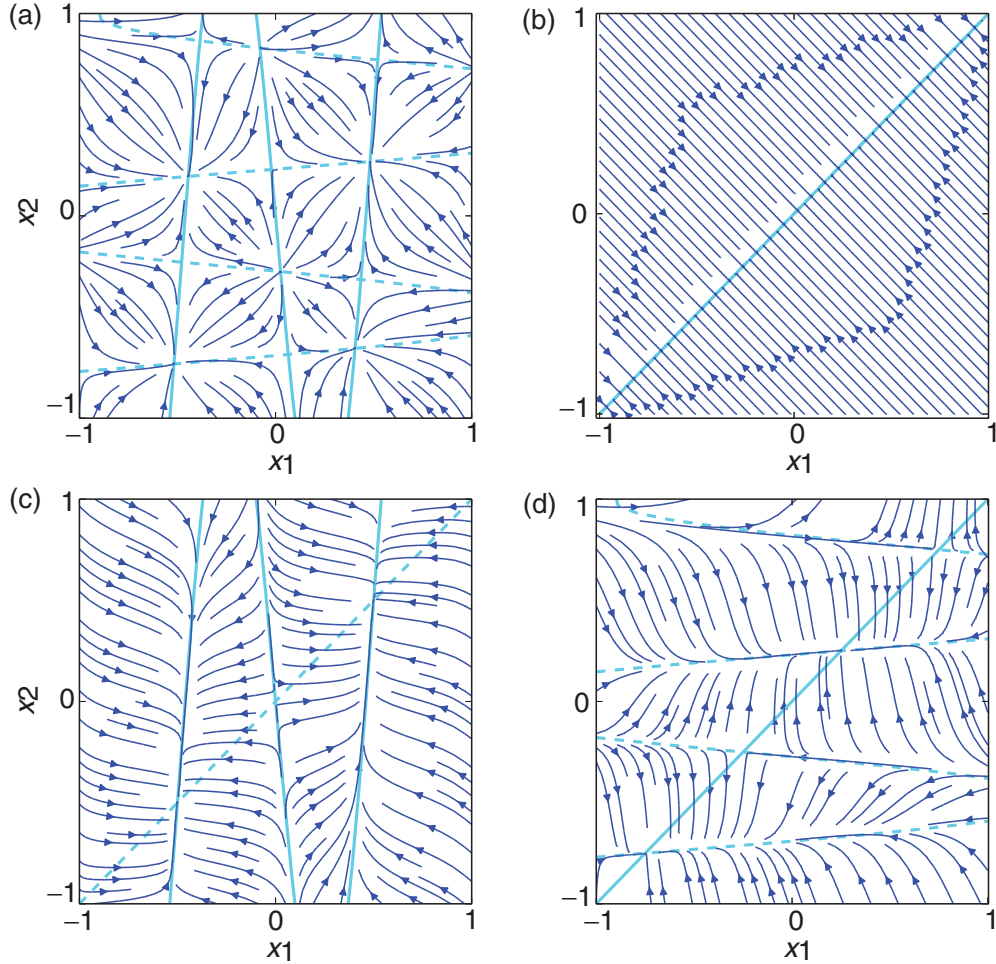


FIG. 6. (Color online) Plots of the vector field  $\mathbf{v}_s(\mathbf{x})$  (dark lines) and nullclines (light lines) for motor 1 (solid lines) and motor 2 (dashed lines) in (a) the fully attached state ( $s = 11$ ), (b) the fully detached state ( $s = 00$ ), (c) the particles-one attached state ( $s = 10$ ), and (d) the particles-two attached state ( $s = 01$ ). Both particles move in the same sinusoidal potential modulo a phase shift. The parameter values are  $D = \ell = 1$ ,  $\bar{\Omega} = 10$ ,  $\kappa = 8$ , and  $z = 0$ .

necessarily the gradient of a potential. However, examining the vector field  $\mathbf{v}(\mathbf{x})$  yields insight into qualitative features of the system, as we know that for small  $\varepsilon$  the QSS provides an accurate approximation to the full system. For  $\varepsilon \rightarrow 0$  the stochasticity resulting from state transitions is absorbed into the deterministic part of the system. Therefore, provided we have chosen parameter values such that  $\mathbf{v}(\mathbf{x})$  is not at a bifurcation point, there exist small but nonzero values of  $\varepsilon$  for which we expect the full system and the QSS system to share the same metastable states.

A visual comparison of  $\mathbf{v}(\mathbf{x})$  with the stochastic trajectories of the full system reveals that the QSS accurately predicts the metastable states for a range of  $\varepsilon$  values. We show this in Fig. 8, where it can be seen that even for relatively large values of  $\varepsilon$  the particle fluctuates near the fixed points of  $\mathbf{v}(\mathbf{x})$ . Note that the initial condition for the stochastic trajectories is in the basin of attraction for a fixed point of  $\mathbf{v}_{11}$  but the stochastic trajectories evolve away from this fixed point towards fixed points of  $\mathbf{v}$ . In Fig. 9 we show the same for  $\kappa = 0.1$ . In this case  $\mathbf{v}_{11}$  and  $\mathbf{v}$  nearly agree but the QSS was needed to establish this fact. In both cases the QSS vector fields appears to represent a small perturbation of the exact dynamics. We would expect that if

there exists a quasipotential, such as one derived from a WKB approximation, the QSS would approximate the corresponding gradient vector field. Our numerical simulations for other transitions rates indicate that the QSS reduction is a reliable method for determining the metastable states of the coupled ratchet system.

Thus far, for the coupled system we have only demonstrated that the QSS approximation accurately predicts the behavior of the system over short time scales. While this is indeed interesting in its own right, the results for the single motor, and specifically those presented in Fig. 3, suggest that one can also use the QSS approximation to determine the mean velocity of the coupled ratchets as a function of biophysical parameters. Let  $v^c$  denote the average velocity of the center of mass for the coupled system. In Fig. 10(a) we show numerical results comparing the mean velocity of the full system with that of the SDE corresponding to Eq. (5). For the sake of illustration, we consider asymmetric transition rates and homogenous perturbations from detailed balance. It can be seen that the velocity of the center of mass is a monotonically increasing function of spring stiffness  $\kappa$  in both cases and there is reasonable quantitative agreement.

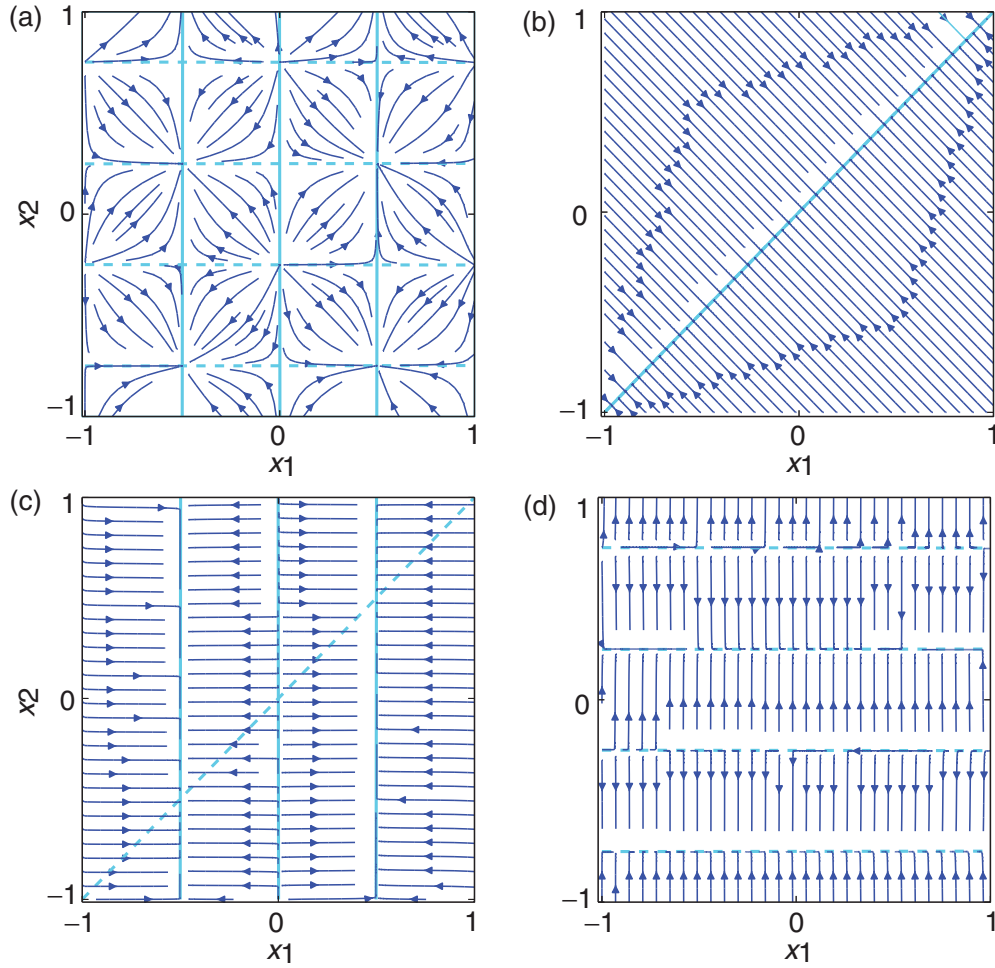


FIG. 7. (Color online) Same as in Fig. 6 with  $\kappa = 0.1$ .

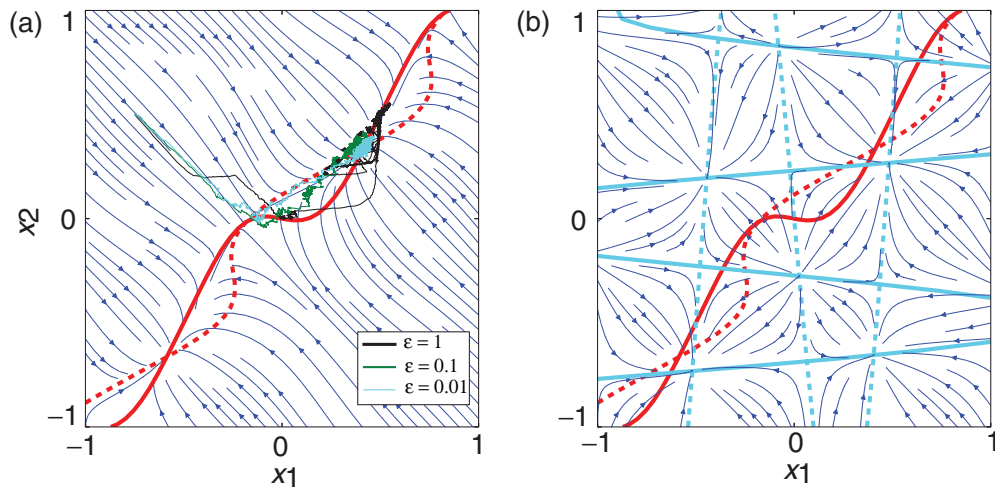


FIG. 8. (Color online) (a) Stochastic trajectories of the full system superimposed on the QSS vector field  $\mathbf{v}(\mathbf{x})$  for various values of  $\varepsilon$ . The nullclines are shown as thicker (red) curves for motor 1 (solid lines) and motor 2 (dashed lines). The parameters used are  $\kappa = 8$ ,  $D = 1$ , and  $\bar{\Omega} = 10$ . The stochastic trajectories were generated using the same algorithm as in Fig. 5 for  $T = 10$  ms with  $dt = 0.001$  ms and all three simulations are with the initial condition  $\mathbf{x}(0) = (-0.75, 0.5)$ . Note that to make the figure readable  $T$  was chosen so that we only see convergence to a single metastable state. This is in contrast to Fig. 5, where the transitions between metastable states can be observed. (b) The QSS nullclines (dark thick curves) superimposed on the vector field  $\mathbf{v}_{11}(\mathbf{x})$  and nullclines (thick light curves) for the fully attached state of the full system.

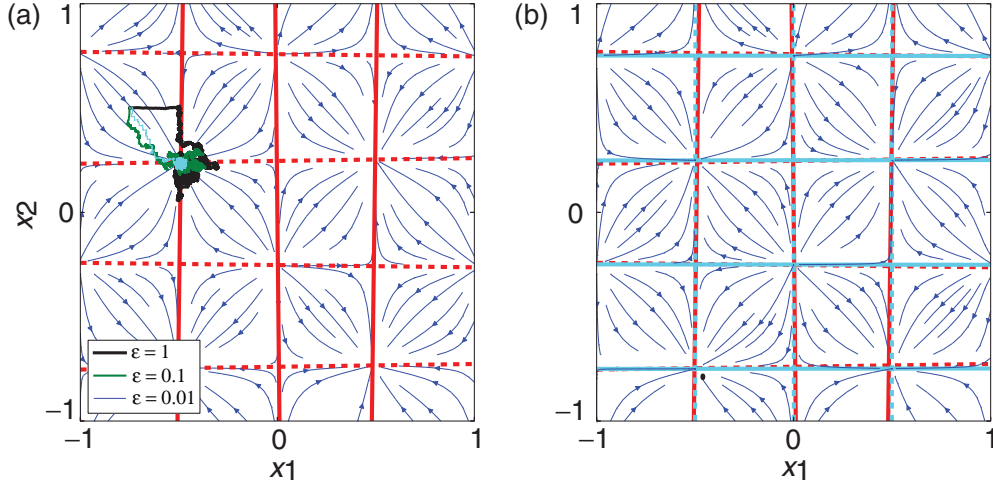


FIG. 9. (Color online) Same as in Fig. 8 with  $\kappa = 0.1$ .

Figure 10(b) shows convergence to the QSS velocity as  $\varepsilon \rightarrow 0$  for fixed  $\kappa$ . Our results are consistent with a previous study of the strain-independent coupled ratchet model [10]. Note that in models of coupled molecular motors that include strain-dependent unbinding [25], one finds that increasing  $\kappa$  reduces the velocity.

We now show how one can derive an expression for the velocity of the center of mass by utilizing the symmetries of Eq. (5) to obtain a system that is  $\ell$  periodic in the horizontal direction. First, given the assumptions on  $\omega_{\text{on}}^{(i)}$ ,  $\omega_{\text{off}}^{(i)}$ , and  $f_i(x_i)$ , it follows that  $f_i(x_i)\sigma_i(x_i)$  is  $\ell$  periodic in  $x_i$ . Hence, in the absence of elastic coupling the original system is doubly periodic with respect to the transformations

$$x_1 \mapsto x_1 + n_1\ell, \quad x_2 \mapsto x_2 + n_2\ell$$

for arbitrary integers  $(n_1, n_2)$ . In the presence of elastic coupling this symmetry reduces to

$$x_1 \mapsto x_1 + n\ell, \quad x_2 \mapsto x_2 + n\ell,$$

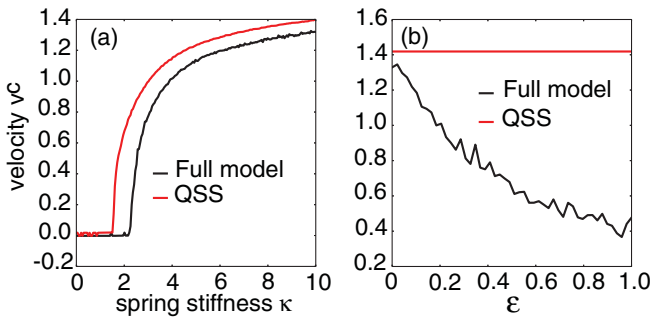


FIG. 10. (Color online) (a) Average velocity  $v^c$  as a function of  $\kappa$  for the full model and QSS. Simulations for the full and reduced system were performed using Euler’s method for the SDE, taking into account switching in the full system. Here we have used the piecewise linear potentials with a  $\ell/4$  phase offset and homogenous perturbations from detailed balance shown in (a). The parameters used are  $D = 1$ ,  $a = 0.1$ , and  $\varepsilon = 0.001$ . (b) Average velocity  $v^c$  as a function of  $\varepsilon$  showing convergence to the QSS velocity as  $\varepsilon \rightarrow 0$ . The same parameter values are used and  $\kappa = 8$ .

i.e.,  $n_1 = n_2$ . Under the latter symmetry  $v_i(\mathbf{x})$  is invariant. Hence, defining

$$\xi_1 = \frac{1}{\sqrt{2}}(x_1 - x_2), \quad \xi_2 = \frac{1}{\sqrt{2}}(x_1 + x_2),$$

the  $v_i$  are invariant under the transformation

$$\xi_1 \rightarrow \xi_1 + n\ell, \quad \xi_2 \rightarrow \xi_2.$$

Therefore, consider the change of variables  $\mathbf{x} \rightarrow \boldsymbol{\xi} = (\xi_1, \xi_2)$ . In matrix notation the appropriate transformation is given by

$$\mathcal{R} = \begin{pmatrix} 1 & -1 \\ 1 & 1 \end{pmatrix}$$

so that  $\boldsymbol{\xi} = \mathcal{R}\mathbf{x}$ . Now Eq. (5) can be rewritten as

$$\frac{\partial \tilde{u}}{\partial t} = -\nabla \cdot [\tilde{\mathbf{v}}(\boldsymbol{\xi})\tilde{u}] + D\nabla^2 \tilde{u}, \quad (8)$$

where  $\tilde{u}(\boldsymbol{\xi}, t) = u(\mathcal{R}^{-1}\boldsymbol{\xi}, t)$  and

$$\tilde{\mathbf{v}}(\boldsymbol{\xi}) = \mathcal{R}\mathbf{v}(\mathcal{R}^{-1}\boldsymbol{\xi}).$$

We simplify notation by dropping the tildes in the remainder of this section. Note that  $\xi_1$  is proportional to the center of mass, while  $\xi_2$  measures the displacement of the spring from equilibrium. It is also worth noting that after this transformation we have the useful relation

$$v_2(\boldsymbol{\xi}) = -2\kappa(\xi_2 - z) - v_1(\boldsymbol{\xi})$$

and, as we would expect,

$$\lim_{\xi_2 \rightarrow -\infty} v_2(\boldsymbol{\xi}) > 0, \quad \lim_{\xi_2 \rightarrow \infty} v_2(\boldsymbol{\xi}) < 0.$$

We introduce the reduced density

$$\hat{u}(\boldsymbol{\xi}, t) = \sum_{n=-\infty}^{\infty} u(\xi_1 + n\ell, \xi_2, t).$$

Linearity and the periodicity of  $\mathbf{v}$  guarantee that  $\hat{u}$  satisfies Eq. (8) on the strip  $[0, \ell] \times \mathbb{R}$ , subject to the periodic boundary conditions

$$\hat{u}(0, \xi_2, t) = \hat{u}(\ell, \xi_2, t).$$



The fact that the domain of  $\xi_1$  is finite along with the limiting behavior of  $\xi_2$  guarantees that there is a time-independent steady-state solution  $\hat{u}^{SS}(\xi) = \hat{u}(\xi, t)$ . We consider the probability flux

$$\hat{J}(\xi, t) = v(\xi)\hat{u} - D\nabla\hat{u}.$$

At steady state the horizontal component of the flux satisfies

$$J_1^{SS}(\xi) = v_1(\xi)\hat{u}^{SS}(\xi) - D\frac{\partial}{\partial\xi_1}\hat{u}^{SS}(\xi) \quad (9)$$

and velocity of the center of mass is then given by

$$v_{QSS}^c = \int_{[0, \ell] \times \mathbb{R}} J_1^{SS}(\xi) d\xi. \quad (10)$$

Equation (10) is the analogous expression to Eq. (2) for the coupled ratchet system. Although it is difficult to obtain an explicit formula for the velocity, Eq. (10) should provide a computationally efficient method for numerically solving for  $v^c$  as a function of biophysical parameters for a wide variety of models. We hope to explore this particular aspect in future work.

#### IV. DISCUSSION

To summarize, we have shown that the QSS reduction is a useful tool for obtaining qualitative information about flashing ratchets. When applied to a single-particle flashing ratchet, the QSS reduction yields a single effective potential describing the motion of the system, relating two fundamental mechanisms for generating noise-induced transport in periodic media. The QSS reduction converts a spatially periodic stochastic hybrid system, in which nonequilibrium perturbations in the discrete dynamics give rise to directed transport, to a continuous-time stochastic process where information about the nonequilibrium perturbations is contained in an aperiodic forcing term. The latter system is significantly easier to study. We derived the relationship between mean particle velocity and perturbations from detailed balance, namely, that the velocity is a monotonic function of the amplitude of the perturbations when they are localized and unimodal when they are homogenous. While this relationship has previously been shown for specific transition rates, we are not aware of a more general derivation.

In general, identifying metastable states in stochastic hybrid systems is a difficult problem. For the single on-off flashing

ratchet, it is clear that the metastable states are located at the minima of the nontrivial potential and the QSS accurately preserves this. For a system of two coupled flashing ratchets the situation is more complicated and an inspection of the individual potentials does not allow one to identify the metastable states. However, such states can be determined from the effective vector field obtained using a QSS reduction. The existence and distribution of metastable states and the resulting asynchrony in the stepping of the two motors or, alternatively, a single motor consisting of two heads, strongly depend on the elasticity of the tether. This is consistent with previous studies of elastically coupled motors, in which space is discretized [25–27,30]. We have also presented numerical results that suggest that the QSS preserves the velocity of the system and derived an expression for the velocity of the center of mass.

There are a number of possible extensions of our work. For example, one could extend the analysis of two coupled ratchets to larger systems of collective transport that go beyond mean field theory. In mean field models one often takes the coupling between particles to be rigid. However, this simplification breaks down for a finite number of particles leading to analytically intractable systems. As a result, few studies have considered how elastic coupling effects collective transport by many molecular motors. The QSS reduction of a system of  $N$  two-state flashing ratchets will yield a Brownian particle evolving in an  $N$ -dimensional domain. In order to extend our analysis to systems with  $N > 2$ , one would need to specify how the motors are coupled. For example, nearest-neighbor coupling between motors would likely yield different dynamic behavior than coupling to a single cargo. Hence extensions of our analysis require one to be more specific about the corresponding physical or biological system of interest. It would also be of interest to carry out a more general mathematical investigation of the relationship between stochastic hybrid systems and the continuous system resulting from the QSS reduction. Obtaining a quasipotential from a WKB approximation is useful for escape problems in stochastic hybrid systems in which noise is weak and the interval state dynamics are deterministic. However, when there is a strong diffusion within the individual states, the QSS may be sufficient to identify the import features of the dynamics. We are interested in what features of a stochastic hybrid system are preserved and in obtaining bounds on the values of  $\varepsilon$  for which the dynamics are equivalent up to homotopy.

- 
- [1] P. C. Bressloff, *Stochastic Processes in Cell Biology* (Springer, Berlin, 2014).
  - [2] P. Reimann, *Phys. Rep.* **361**, 57 (2002).
  - [3] J. Prost, J.-F. Chauwin, L. Peliti, and A. Ajdari, *Phys. Rev. Lett.* **72**, 2652 (1994).
  - [4] C. S. Peskin, G. B. Ermentrout, and G. Oster, in *Cell Mechanics and Cellular Engineering*, edited by V. Gow (Springer, New York, 1995).
  - [5] A. Parmeggiani, F. Jülicher, A. Ajdari, and J. Prost, *Phys. Rev. E* **60**, 2127 (1999).
  - [6] F. Jülicher, A. Ajdari, and J. Prost, *Rev. Mod. Phys.* **69**, 1269 (1997).
  - [7] D. Keller and C. Bustamante, *Biophys. J.* **78**, 541 (2000).
  - [8] R. Lipowsky and S. Klumpp, *Physica A* **352**, 53 (2005).
  - [9] A. Kolomeisky and M. Fisher, *Annu. Rev. Phys. Chem.* **58**, 675 (2007).
  - [10] D. Dan, A. M. Jayannavar, and G. I. Menon, *Physica A* **318**, 40 (2003).
  - [11] J. Howard, *Mechanics of Motor Proteins and the Cytoskeleton* (Sinauer, Sunderland, 2001).
  - [12] Y. Sowa and R. M. Berry, *Quart. Rev. Biophys.* **41**, 103 (2008).
  - [13] T. Guerin, J. Prost, and J.-F. Joanny, *E. Phys. J. E* **34**, 1 (2011).

- [14] T. Guérin, J. Prost, and J.-F. Joanny, *Phys. Rev. E* **84**, 041901 (2011).
- [15] J. G. Orlandi, C. Blanch-Mercader, J. Brugués, and J. Casademunt, *Phys. Rev. E* **82**, 061903 (2010).
- [16] S. Klumpp, C. Keller, F. Berger, and R. Lipowsky, *Multiscale Modeling in Biomechanics and Mechanobiology* (Springer, Berlin, 2015), pp. 27–61.
- [17] C. S. Peskin and T. C. Elston, *SIAM J. Appl. Math.* **60**, 842 (2000).
- [18] R. E. L. DeVille and E. Vanden-Eijnden, *Commun. Math. Sci.* **5**, 431 (2007).
- [19] M. H. A. Davis, *J. R. Stat. Soc. Ser. B* **46**, 353 (1984).
- [20] T. C. Elston, *J. Math. Biol.* **41**, 189 (2000).
- [21] J. M. Newby and P. C. Bressloff, *Bull. Math. Biol.* **72**, 1840 (2010).
- [22] S. A. McKinley, A. Athreya, J. Fricks, and P. R. Kramer, *J. Theor. Biol.* **305**, 54 (2012).
- [23] E. M. Craig, M. J. Zuckermann, and H. Linke, *Phys. Rev. E* **73**, 051106 (2006).
- [24] A. Mogilner, T. Elston, H. Wang, and G. Oster, in *Computational Cell Biology*, edited by C. Fall, E. S. Marland, J. M. Wagner, and J. J. Tyson (Springer, New York, 2002), Chap. 13.
- [25] F. Berger, C. Keller, R. Lipowsky, and S. Klumpp, *Cell. Mol. Bioeng.* **6**, 48 (2013).
- [26] F. Berger, C. Keller, S. Klumpp, and R. Lipowsky, *Phys. Rev. Lett.* **108**, 208101 (2012).
- [27] S. Klumpp and R. Lipowsky, *Proc. Natl. Acad. Sci. USA* **102**, 17284 (2005).
- [28] S. D. Lawley, J. C. Mattingly, and M. C. Reed, *Commun. Math. Sci.* **12**, 1343 (2014).
- [29] P. C. Bressloff and J. M. Newby, *Phys. Rev. E* **89**, 042701 (2014).
- [30] H. Lu, A. K. Efremov, C. S. Bookwalter, E. B. Krementsova, J. W. Driver, K. M. Trybus, and M. R. Diehl, *J. Biol. Chem.* **287**, 27753 (2012).